ISSN 1075-7015, Geology of Ore Deposits, 2013, Vol. 55, No. 8, pp. 648–662. © Pleiades Publishing, Ltd., 2013.
Original Russian Text © L.A. Pautov, M.P. Popov, Yu.V. Erokhin, V.V. Khiller, V.Yu. Karpenko, 2012, published in Zapiski Rossiiskogo Mineralogicheskogo Obshchestva, 2012, No. 6, pp. 43–62.

Mariinskite, $BeCr_2O_4$, a New Mineral, Chromium Analog of Chrysoberyl[1]

L. A. Pautov[a, 2], M. P. Popov[b], Yu. V. Erokhin[b], V. V. Khiller[b], and V. Yu. Karpenko[a]

[a] *Fersman Mineralogical Museum, Russian Academy of Sciences, Leninsky pr. 18–2, 119071 Moscow, Russia*

[b] *Institute of Geology and Geochemistry, Ural Division, Russian Academy of Sciences, Pochtovyi per. 7, Yekaterinburg, 620151 Russia*

Received March 19, 2012

Abstract—A new mineral, mariinskite, $BeCr_2O_4$, the chromium analog of chrysoberyl, has been found at the Mariinsky (Malyshevo) deposit, the Ural Emerald Mines, the Central Urals, Russia. The mineral is named after its type locality. It was discovered in chromitite in association with fluorphlogopite, Cr-bearing muscovite, eskolaite, and tourmaline. Mariinskite occurs as anhedral grains ranging from 0.01 to 0.3 mm in size; in some cases it forms pseudohexagonal chrysoberyl-type twins. The mineral is dark-green, with a pale green streak; the Mohs' hardness is 8.5, microhardness VHN = 1725 kg/mm^2. D_{meas} = 4.25(2) g/cm^3, D_{calc} = 4.25 g/cm^3. Microscopically, it is emerald-green, pleochroic from emerald-green (γ) to yellow-green (β) and greenish yellow (α). The new mineral is biaxial (+), γ = 2.15(1), β = 2.09(3), and α = 2.05(1), $2V_{meas}$ = 80 ± (10)°, $2V_{calc}$ = 80.5°. In reflected light, it is gray with green reflections; R_{max} (589) = 12.9%; R_{min} (589) = 12.3%, and there are strong, internal green reflections. The strongest absorption bands in the IR spectrum are as follows (cm^{-1}): 935, 700, 614, 534. Space group *Pnma*, *a* = 9.727(3), *b* = 5.619(1), *c* = 4.499(1) Å, *V* = 245.9(3) Å^3, *Z* = 4. The strongest reflections in the X-ray powder diffraction pattern are as follows (*d* Å, *I*, *hkl*): 4.08(40)(101), 3.31(90)(111), 2.629(50)(301), 2.434(50)(220), 2.381(40)(311), 2.139(60)(221), 1.651(100)(222). The average chemical composition of mariinskite (electron microprobe, wt %) is as follows: BeO 16.3, Al_2O_3 23.89, Cr_2O_3 58.67, Fe_2O_3 0.26, V_2O_3 0.26, TiO_2 0.61, total is 99.98. The empirical formula, calculated on the basis of four O atoms is $Be_{1.03}(Cr_{1.22}Al_{0.74}Ti_{0.01}Fe_{0.01}V_{0.01})_{1.99}O_4$. The compatibility index $1 - (K_p/K_c)$, 0.019, is excellent. The type specimens are deposited in the Fersman Mineralogical Museum, Russian Academy of Sciences, Moscow, and the Ural Geological Museum, Yekaterinburg, Russia.

DOI: 10.1134/S1075701513080096

INTRODUCTION

A new mineral with the idealized formula $BeCr_2O_4$ was found in chromitite from the Mariinsky (Malyshevo) deposit, Ural Emerald Mines (Fig. 1). The mineral was named mariinskite after its type locality.

Mariinskite, $BeCr_2O_4$, is a chromium analog of chrysoberyl, $BeAl_2O_4$, whose well-studied structure was repeatedly refined (Bragg and Brown, 1926; Farrell et al., 1963; Dudka et al., 1985). Chrysoberyl crystallizes in the olivine structure type characterized by slightly distorted hexagonal packing, where half of the variable-symmetry octahedral vacancies of *M1* and *M2* types are occupied by Al, and 1/8 of tetrahedral sites are occupied by Be atoms. In the second half of 19th century, J.J. Ebelmen synthesized crystalline phase with a composition of $BeCr_2O_4$, and Mallard (1888) suggested isomorphism in the series $BeAl_2O_4$–$BeCr_2O_4$. Using X-ray powder diffraction, Weir and Van Valkenburg (1960) verified the identical structure of synthetic members of this solid solution series and determined the orthorhombic unit-cell dimensions of the end member $BeCr_2O_4$: *a* = 9.792, *b* = 5.663, *c* = 4.555 Å. The phases of this system in a wide range of composition have currently been synthesized and studied in various details (Newnham et al., 1964; Santoro and Newnham, 1964; Bukin et al., 1981; Rabadanov and Dudka, 1998; Scalvi et al., 2005; Vinnik et al., 2008; Trindade et al., 2010; Gromalova, 2010; Urusov et al., 2011). In a number of publications, it has been stated that the Cr^{3+} substituting for Al in the structure of chrysoberyl occupies the larger, distorted octahedral site *M2* more readily than smaller and more regular octahedron *M1*, so that ratio of Cr^{3+} at sites *M1* and *M2* is 1 : 2 to 1 : 3 (Rabadanov and Dudka, 1998; Rager et al., 1998; Urusov et al., 2011). However, in natural, Cr-bearing chrysoberyl, such distribution of Cr by octahedral sites is not always detectable; sometimes, site *M1* is preferable for occupation by this element (Urusov et al., 2011). In the last few years, great efforts aimed at atomistic modeling of structures in the $BeAl_2O_4$–$BeCr_2O_4$ system have allowed a substantial approach to the theoretical cal-

[1] A new mineral, mariinskite, and its name were recommended by the Commission on New Minerals Russian Mineralogical Society and approved by the Commission on New Minerals, Nomenclature, and Mineral Classification of the International Mineralogical Association on September 1, 2011 (IMA no. 2011-057.

[2] Corresponding author L.A. Pautov. E-mail: pla58@mail.ru

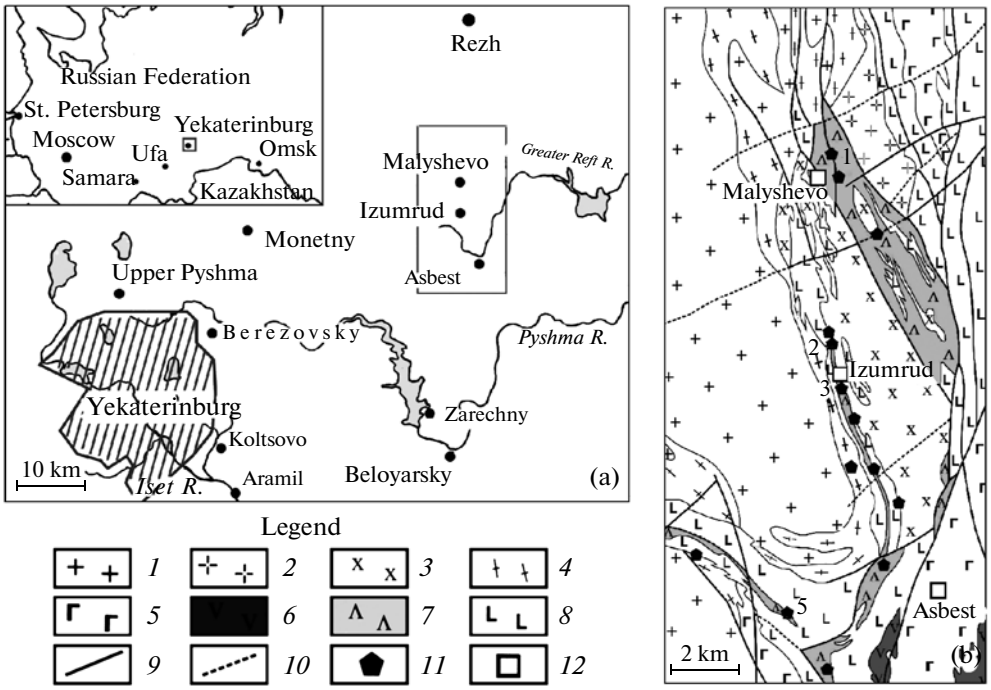

Fig. 1. (a) Location of the Ural Emerald Mines; (b) geological map of the area adjacent to the Mariinsky deposit, modified after F.F. Zolotukhin and V.I. Skobelkin.

(*1*) Leuco- and mesocratic granitic rocks of the Adui pluton; (*2*) leucogranite of the Malyshevo pluton; (*3*) diorites of the Lesozavodsky pluton; (*4*) granite-gneiss framework of the Adui pluton; (*5*) gabbronorite of the Bazhenovo ophiolite complex; (*6*) harzburgite, websterite, and serpentinite of the Bazhenovo ophiolite complex; (*7*) talc metasomatic rock replaced ultramafic rocks with phlogopite schist complexes; (*8*) volcanic–sedimentary sequence; (*9–10*) fault and melange zones: (*9*) proved, (*10*) inferred; (*11*) emerald–beryl deposits and occurrences. Numerals mark the largest deposits (initial names are given; names given after renaming in 1927 are placed in parentheses): (1) Mariinsky (Malyshevo), (2) Troitsky (Pervomaisky), (3) Sretensky (Sverdlov). (4) Cheremshansky; (5) Khitny Mine (Krasnoarmeisky); (*12*) settlement.

culation of many physical properties of compounds in this system (Eremin, 2009; Gromalova et al., 2011).

Chromium is a frequent isomorphic admixture in natural chrysoberyl from deposits related to ultramafic rocks (Fig. 2). Cr-bearing chrysoberyl, changing in color from emerald-green in daylight to wine-red in artificial light, was found for the first time in the the Ural Emerald Mines in 1830s. The first mentions of the Ural chrysoberyl were made by Ya.V. Kakovin and L.A. Perovsky (Von Pott, 1842); Rose (1839) gave the first mineralogical description. Upon the proposal by N. Nordenskiöld, this gem-quality variety of chrysoberyl was named alexandrite, in honor of the heir to the Russian crown, the future emperor Alexander the Second (Von Pott, 1842). Fersman (1920), Avdonin and Polenov (2004), and Schmetzer (2010) described the history of the discovery and study of alexandrite. Avdeev (1842) and Shubin (1843) were the first to determine the chemical composition of chrysoberyl from the Ural Emerald Mines and revealed 0.36 and 0.93 wt % Cr_2O_3. These data are consistent with later chemical analyses of the Ural alexandrite (Vlasov and Kutukova, 1960; Schmetzer, 2010). The Cr content in alexandrite from other deposits related to ultramafic rocks ranges from 0.0*n* to 1 wt % Cr_2O_3 (Gübelin, 1976; Franz et al., 1996; Basilio et al., 2000; Downes and Bevan, 2002; Trindade et al., 2010; Schmetzer et al., 2011). The highest Cr content (1.36 wt % Cr_2O_3) in chrysoberyl from Dowerin, Australia was published by Downes and Bevan (2002). Chrysoberyl from occurrences unrelated to ultramafic rocks, for example, pegmatite in the Kerala state, India (Soman and Nair, 1985; *Geology* ..., 2005); Golden in Colorado, the United States (Waldschmidt and Gaines, 1939); and Belvis de Monroy in Spain (Merino et al., 2010), as a rule, are depleted in Cr (<0.1 wt % Cr_2O_3). Thus, the concentration of Cr in natural chrysoberyl is lower by one to one and half order than in mariinskite (Fig. 2).

TYPE LOCALITY AND MINERAL ASSEMBLAGE

The Ural Emerald Mines are located on the eastern slope of the Central Urals in the vicinity of the town of Asbest, approximately 60 km southeast of Yekaterinburg, as a group of emerald–beryl deposits extending for 25 km in the meridional direction (Fig.1). The discovery and mining of the Emerald Mines started in 1830, when M.S. Kozhevnikov found emerald crystals

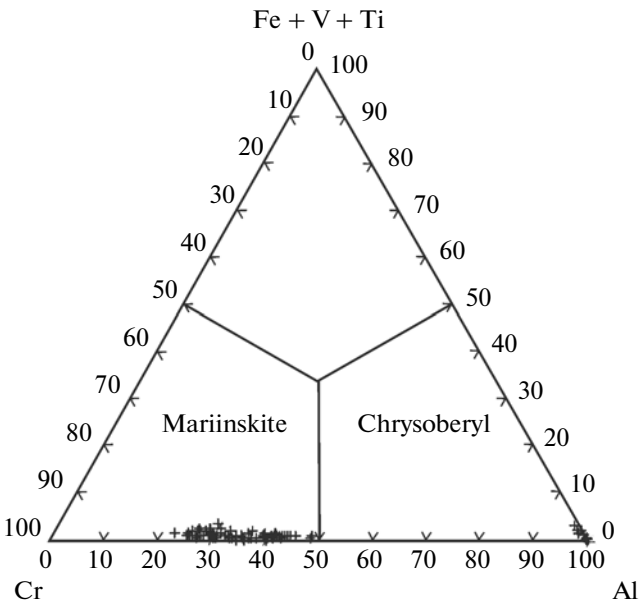

Fig. 2. Chemical composition of minerals pertaining to the mariinskite–chrysoberyl series plotted in the ternary diagram of Cr, Fe + Ti + V, Al end members, mol %. The compositions of mariinskite are our data; the compositions of chrysoberyl were taken from the literature: Ural Emerald Mines (Avdeev, 1842; Shubin, 1843; Vlasov and Kutukova, 1960); Lake Manyara, Tanzania (Gübelin, 1976); Kerala, India (Soman and Nair, 1985); Dowerin, Australia (Downes and Bevan, 2002); Franqueira, Spain (Franz et al., 1996); Belvis de Monroy, Spain (Merino et al., 2010); Minas Gerais, Brasil (Trindade et al., 2010). The compositions of only Cr-bearing chrysoberyl are given.

on the bank of the Tokovaya River. In 1831, as ordered by Kakovin, the mining started at this locality and soon the Sretensky Mine was commissioned. In 1832, Troitsky Mine was founded 4 km north of the first mine, and in the following year the Mariinsky deposit, located 8.5 km north of the Sretensky Mine, was discovered. Archival materials on the Ural Emerald Mines were published by Fersman (1923). The history of the opening of the mines' location has been referenced in a large number of publications (Fersman, 1913, 1920; Vlasov and Kutukova, 1960; Zolotukhin, 1996); Avdonin and Polenov, 2004; and Popov et al., 2008). In 1927, the Ural Emerald Mines were renamed (Fig. 1). In geology and petrography, the area of the Emerald Mines is divided into the western zone, occupied by the Adui granitic pluton; the eastern zone, composed of the Bazhenovo ophiolite complex; and the central zone, consisting of metamorphosed volcanic–sedimentary sequences and utramafic rocks cut through by porphyritic diorite dikes (Zolotukhin, 1999). All beryl deposits and occurrences, including those containing emerald, are localized in the central block and related to the contact of the Adui granitic pluton with the Paleozoic metamorphic sequence. The age of zircon, monazite, and mica from the Adui Granite is estimated at 291 ± 8 Ma (Krasnobaev et al., 2006), 256 ± 0.6 Ma (Fershtater et al., 2003), and 241–255 Ma (Smirnov et al., 2006), respectively. Beryllium mineralization is mainly hosted in quartz–plagioclase veins and bodies of phlogopite schists, controlled by near-meridional faults, foliation zones, and by the screening effect of porphyritic diorite dikes (Vlasov and Kutukova, 1960; Zolotukhin, 1996; Kupriyanova, 2004; Bidny, 2012).

The Mariinsky deposit, where mariinskite has been found, is the largest among the Ural Emerald Mines and is located in the northern segment of the metamorphic wedge between the Adui and Malyshevo granitic plutons. Emerald-bearing phlogopite schists develops after serpentinite melange. The richest ore bodies are located in the thick, talc schist zones (Kupriyanova, 2004). Serpentinite blocks are less favorable for emerald mineralization, but they contain chromitite lenses, in one of which the new mineral has been revealed. Mariinskite was identified in the specimen of chromitite, which had been kindly placed at our disposal by Valery Mikhailovich Vydrin. The specimen came from level +60 m, Southern Mine, Mariinsky deposit. Fersman (1926) was the first to note fine chromite grains in actinolite from the Troitsky Mine. Chromite from the Emerald Mines was also described by Vertushkov (1937), Vlasov and Kutukova (1960), and Zhernakov (2004).

The studied specimen of chromitite is a fine- to medium-grained brown rock pierced by numerous, variously oriented veinlets composed of green mica. The major minerals are chromite, fluorphlogopite, and Cr-bearing muscovite; mariinskite is minor; eskolaite, tourmaline supergroup minerals, fluorapatite, and zircon are accessories. Chromite is present in two varieties: isolated unfaced grains of Al-rich chromite I (end-member composition, mol %: 54 $FeCr_2O_4$, 23 $MgAl_2O_4$, 18 $MgCr_2O_4$, 3 $MnAl_2O_4$, 1 $ZnAl_2O_4$, 1 FeV_2O_4) and a matrix of low-Al chromite II (63 $FeCr_2O_4$, 24 $MgCr_2O_4$, 7 $MgAl_2O_4$, 3 $MnAl_2O_4$, 1 $ZnAl_2O_4$, 1 FeV_2O_4). Chromite I is regarded as an earlier mineral, which is replaced with chromite II along fractures. Megascopically, chromite I is dark brown, almost black; in transmitted light, the mineral is translucent, dense red-brown, and is readily polished. Chromite II is light brown and poorly polished; its surface is mottled by small isometric defects. In a thin section, chromite I is practically opaque, while in reflected light it has very strong, light brown internal reflections. This inconsistence in properties is explained by numerous and regularly distributed small cavities in chromite II as negative crystals (octahedra?), which we interpret as dissolution cavities (Fig. 3). The transformation of high-Al spinel into low-Al spinel, with a simultaneous increase in Cr and decrease in Mg contents, is noted in many ultramafic massifs in the Urals (Spiridonov et al., 1997). In the ternary Al–Cr–Fe^{3+} plot, the earlier chromite I falls in the field of chromite from Alpine-type dunite (Plaksenko, 1989); according to the typification of chromite ores, it is

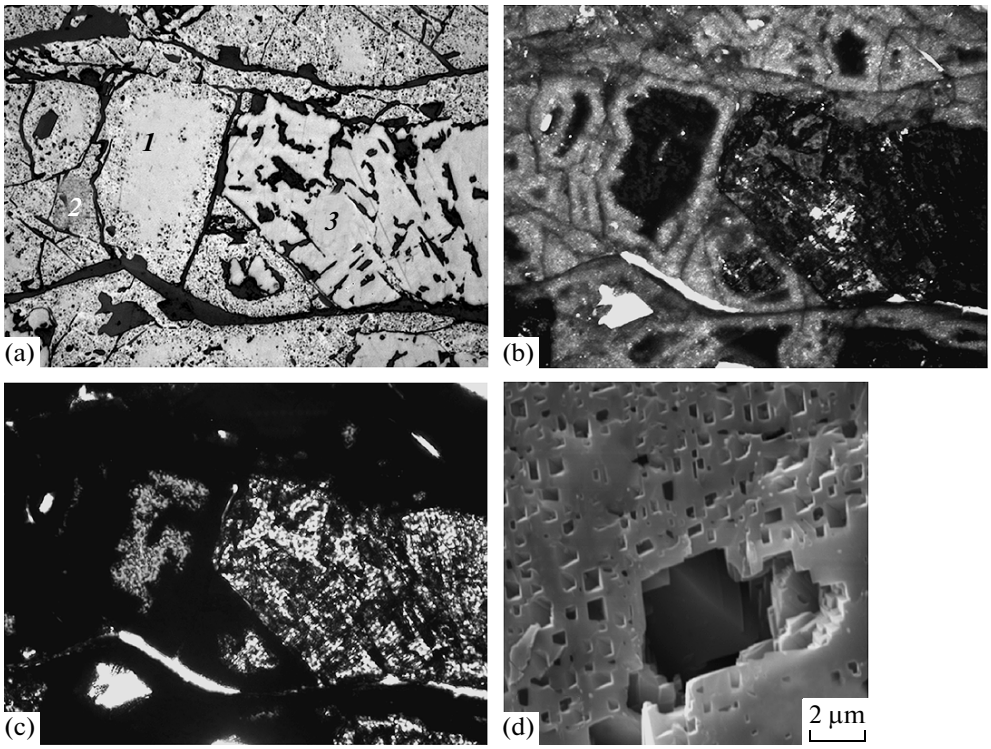

Fig. 3. A grain of mariinskite in aggregate of chromite I, chromite II, and fluorphlogopite: (a) thin polished section, reflected light, normal light: *1*, chromite I; *2*, chromite II; *3*, mariinskite; fluorphlogopite is black; (b) the same area of the thin polished section in reflected light, crossed polars; it is seen that chromite II rims chromite I and its location is controlled by fractures; (c) photomicrograph in transmitted light; it is seen that chromite I is transparent in contrast to opaque chromite II; width of image 330 μm; (d) Secondary electron image of a grain chip of chromite II; numerous cavities as negative crystals are seen. JSM T-100 JEOL SEM, image in secondary electrons.

assigned to the chromites related to dunite–harzburgite and marginal dunite complexes (Sakhnov, 2008).

Veinlets in chromite are composed of light gray fluorphlogopite with greenish tint ($\beta \sim \gamma = 1.569 \pm 0.002$; the end-member composition, mol %: 43 fluorphlogopite $KMg_3AlSi_3O_{10}F_2$, 18 phlogopite $KMg_3AlSi_3O_{10}(OH)_2$, 14 polylithionite $KLi_2AlSi_4O_{10}F_2$, 8 eastonite $KMg_2AlAl_2Si_2O_{10}(OH)_2$, 7 aspidolite $NaMg_3AlSi_3O_{10}(OH)_2$, 6 chromphyllite $KCr_2 \square AlSi_3O_{10}(OH)_2$, and 4 voloshinite $RbLi_{1.5}Al_{0.5}Si_{3.5}O_{10}F_2$) and turquoise-green chromium muscovite ($\beta \sim \gamma = 1.601 \pm 0.002$; the end-member composition, mol %: 44 muscovite $KAl_2 \square AlSi_3O_{10}(OH)_2$, 16 chromphyllite $KCr_2 \square AlSi_3O_{10}(OH)_2$, 10 paragonite $NaAl_2 \square AlSi_3O_{10}(OH)_2$, 10 fluorphologopite $KMg_3AlSi_3O_{10}F_2$, 10 polylithionite $KLi_2AlSi_4O_{10}F_2$, 6 aluminoceladonite $KAlMgnSi_4O_{10}(OH)_2$, and 3 phlogopite $KMg_3AlSi_3O_{10}(OH)_2$). The proportion of micas is highly variable. In some places, fluorphlogopite dominates, while elsewhere, particularly in thin veinlets, chromium muscovite is predominant. As a rule, muscovite occurs as tabular grains and intergrowths of such grains, which are located at selvages of veinlets; the less frequent muscovite sheets are enclosed into the fine-flaked aggregate of phlogopite in the axial part of the veinlets. Micas from the Ural Emerald Mines are typically enriched in Li (Vlasov and Kutukova, 1960; Zhernakov, 1976; Bidny, 2012). According to our few measurements of micas, phlogopite is richer in Li than muscovite.

Tourmaline occurs as dark green columnar and acicular individuals and sheaf-shaped aggregates of these individuals, up to 2–3 cm in length, usually, at the margins of chromite segregations. The zonal structure of tourmaline individuals is detected with an optical microscope and electron microprobe (Fig. 4e). According to the currently adopted nomenclature (Clark et al., 2011; Henry et al., 2011), the individual zones correspond to dravite, fluordravite, and Cr–Al–Mg tourmaline. Eskolaite forms grains with sinuous boundaries and tabular hexagonal crystals up to 200 μm across. They are characterized by growth and sectorial zoning visible in BSE images. The crystal cores are enriched in Al, the concentration of which decreases outward (Fig. 4d; Table 1).

Mariinskite occurs mainly as anhedral fine grains (less than 1 mm) (Figs. 4a, 4c). The grains with linear boundaries are less frequent; however, well-faceted crystals were not observed. Some grains are pseudohexagonal chrysoberyl-type intergrowths (Figs. 4b, 4f, 8a). Individuals of mariinskite are characterized by a complex anatomy

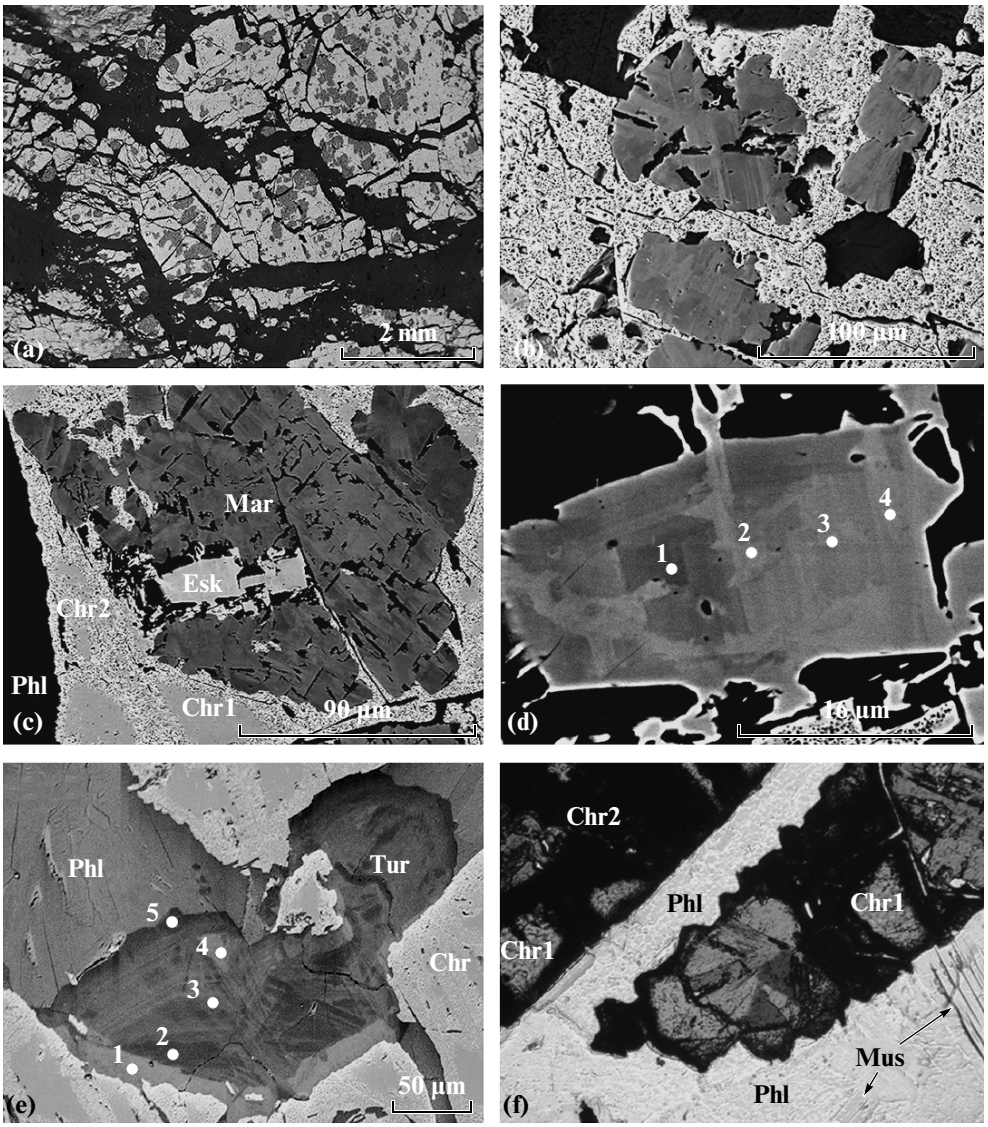

Fig. 4. Minerals associated with mariinskite: (a) BSE image of chromitite with mariinskite, a general view; microbreccia with fragments of chromite (light gray) and mariinskite (gray) cemented by micaceous aggregate (dark gray); (b) BSE image of mariinskite grains (gray) with embedded fluorphlogopite (black) in chromite II; (c) BSE image of eskolaite (Esk) grain in mariinskite (Mar) with numerous inclusions of fluorphlogopite (black) in aggregate of chromite I (Chr1) and chromite II (Chr2); Phl is fluorphlogopite; (d) BSE image of complexly zoned eskolaite grain, a close-up of image (c); numbers correspond to Table 1; (e) BSE image of zonal tourmaline crystal (Tur) among grains of chromite (Chr) and fluorphlogopite (Phl); numbers correspond to Table 2; (f) photomicrograph of chrysoberyl-type trilling of mariinskite in chromite II (Chr2) with relics of chromite I, plane polarized light (Phl) fluorphlogopite, (Mus) muscovite. Width of image is 320 μm.

clearly seen in thin sections and BSE images; growth and sectorial zoning, mottling, and banding are expressed in variable chemical composition in microareas (Figs. 8, 9; Table 3). Blocky crystals and penetration twins often create an intricate pattern in plane sections.

PHYSICAL PROPERTIES AND OPTICAL PARAMETERS

Mariinskite is very dark green, as is seen in fine grains (0.1 mm and smaller) in bright light. The powder (streak) is light green. The luster is strong vitreous. The mineral is transparent in thin sections. The fracture is conchoidal. The Mohs' hardness is 8.5; microhardness VHN measured with a PMT-3 tester loading 150 g (calibrated by NaCl) is 1725 kg/mm^2 (the average of 12 measurements ranging from 1681 to 1771 kg/mm^2). The density determined in the Clerici liquid is 4.25(2) g/cm^3; the calculated density is 4.25 g/cm^3. Mariinskite is not luminescent either in shortwave (254 nm) or longwave (315 nm) UV light or cathode rays. In thin sections, mariinskite is emerald green, though lighter than eskolaite.

Table 1. Chemical composition (wt %) of eskolaite (1–4), chromite I (5) and chromite II (6) associated with mariinskite

Component	Eskolaite				Chromite	
	1	2	3	4	5	6
Al_2O_3	16.51	5.21	6.15	5.52	13.98	5.12
Cr_2O_3	82.54	93.03	91.89	93.12	55.65	64.68
V_2O_3	0.37	0.48	0.27	0.32	0.25	0.19
TiO_2	0.15	0.00	0.00	0.00	0.00	0.00
FeO	0.21	0.23	0.00	0.12	20.06	22.42
MnO	0.24	0.31	0.00	0.54	0.96	0.94
MgO	0.00	0.00	0.00	0.00	8.34	6.09
ZnO	0.25	0.27	0.26	0.26	0.26	0.31
Total	100.26	99.52	99.87	99.87	99.50	99.76

The formulae of eskolaite were calculated on the basis of three O atoms:

(1) $(Cr_{1.52}Al_{0.45}V_{0.01})_{2.00}O_3$, (2) $(Cr_{1.83}Al_{0.15}V^{+3}_{0.01}\ Mn^{+2}_{0.01})_{2.01}O_3$, (3) $(Cr_{1.81}Al_{0.18}V^{+3}_{0.01})_{2.00}O_3$, (4) $(Cr_{1.82}Al_{0.16}V^{+3}_{0.01}\ Mn^{+2}_{0.01})_{2.01}O_3$.
Formulae of chromites calculated on the basis of four O atoms:

(5) chromite I (average of 11 point analyses) $(Fe^{+2}_{0.55}\ Mg_{0.41}\ Mn^{+2}_{0.03}\ Zn_{0.01})_{1.00}(Cr_{1.45}Al_{0.54}V^{+3}_{0.01})_{2.00}O_4$, (6) chromite II (average of 3 point analyses) $(Fe^{+2}_{0.65}\ Mg_{0.32}\ Mn^{+2}_{0.03}\ Zn_{0.01})_{1.01}(Cr_{1.78}Al_{0.21}V^{+3}_{0.01})_{2.00}O_4$. The chemical analyses were carried out on a JCXA-733 SEM equipped with an INCA EDS operated at acceleration voltage 20 kV, current intensity 2 nA; analyzed by L.A. Pautov.
0.00 denotes here and in other tables that the content of the component is below the detection limit by electron microprobe. Analysis numbers 1–4 correspond to numbers in Fig. 4d.

The mineral is pleochroic, from emerald-green on *X*, yellow-green on *Y* to greenish yellow on *Z*. The absorption is $\gamma > \beta > \alpha$.

The mineral is optically biaxial, positive. The measurement of $2V$ on a universal stage failed because of the total internal reflection with a relatively small incline (effect of high refractory indices). $2V$ estimated from curved isogyres is 80 ± 10°; the calculated $2V$ is 80.5°. The extinction, relative to rare linear boundaries of grains and frequent cleavage fractures, is straight, while elongation can be both positive and negative. The extinction is oblique, relative to rare cleavage fractures. Frequently, the extinction is not complete in white light. At the moment of extinction at 589 nm in white light, bright copper or vinaceous color arises. In other sections, an anomalous red color is observed in a diagonal setting relative to extinction. The chrysoberyl-type contact trillings are rare. The intergrowths with sinuous boundaries are more frequent. According to the measurements at the universal

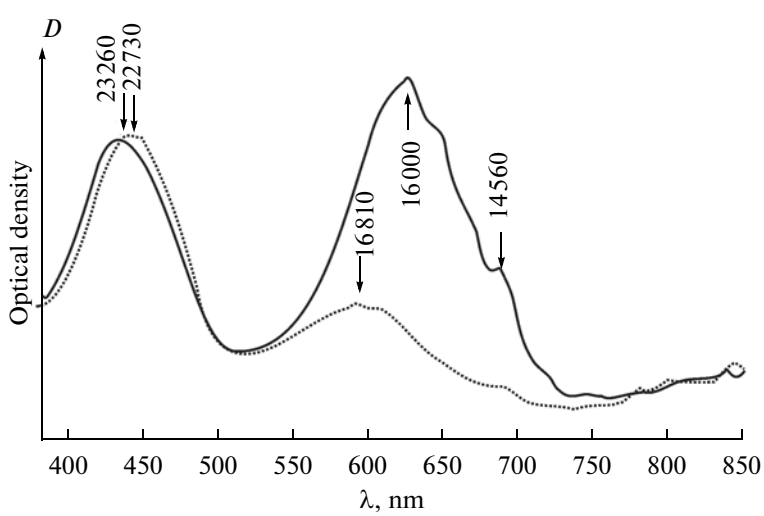

Fig. 5. Optical transmittance spectra of mariinskite. Upper (solid line) and lower (dotted line) spectra correspond to the sections parallel to γ and α, respectively (position of absorption peak is in cm^{-1}).

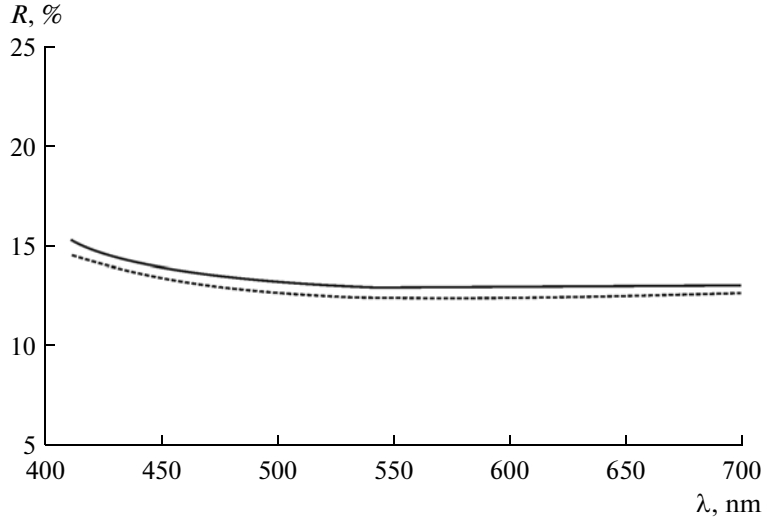

Fig. 6. Reflection spectra of mariinskite: the upper and lower spectra correspond to R_{max} and R_{min}, respectively.

stage, these are penetration twins (unfortunately, the accuracy of these measurements is low). The refractive indices (α and β) of mariinskite were measured in the high-refractive index liquids produced by Cargille Laboratories, the United States, under a sodium lamp (the refractive indices of the liquids are verified with a single-circle goniometer in a cellular prism by the least deviation angle method); γ was determined in the selenium–sulfur alloy: γ = 2.15(1), β = 2.09(3), and α = 2.05.

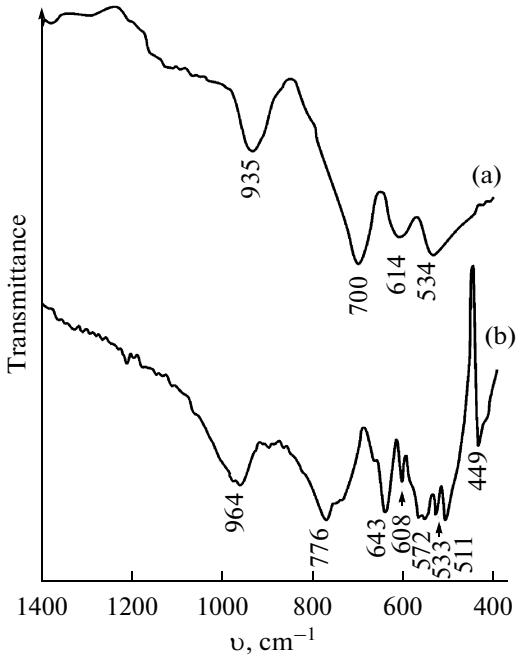

Fig. 7. IR spectra of (a) mariinskite and (b) chrysoberyl from the Mariinsky deposit.

Two broad absorption bands in the region of 430 and 620 nm (on *Z*) and 435 and 600 nm (on *X*) typical of the compounds, whose color is related to Cr^{3+}, are distinct in the optical spectra recorded with a UMSP-50D Opton microscope-spectrophotometer (Fig. 5). In comparison with the position of absorption bands in the spectrum of alexandrite from the Mariinsky deposit (recorded under similar conditions), the indicated absorption bands of mariinskite are shifted to the longwave region of the spectrum; this explains the absence of an alexandrite effect in the new mineral. The shift of the absorption bands is probably caused by larger octahedra MO_6 in mariinskite as compared with alexandrite containing only 0.3 wt % Cr_2O_3.

Mariinskite is readily polished, but notable positive relief relative to chromite and silicates (with which it is intregrown) appears when an insufficiently hard polishing platter is used. In reflected light, the mineral is gray with a very weak bluish tint notable against the brownish-tinted chromite. The reflectance in air ($R_{max(589)}$ = 12.9%, $R_{min(589)}$ = 12.3%) is appreciably lower than that of eskolaite and close to chromite; in immersion liquids, the reflection of mariinskite is lower than that of chromite (II) and close to chromite (I). The reflection spectra of the mineral were obtained on a UMSP-50D microscope-spectrophotometer (SiC as standard) in spots 16 μm in diameter in order to smooth some variations of the mineral reflectance caused by the variable chemical composition in different growth zones. The reflection spectra are gentle, with a weak peak in the blue region (Fig. 6). This is consistent with a visual estimation of the mariinskite color in reflected light. Mariinskite is characterized by very strong internal reflections, which hamper the record of correct reflection spectra. Bireflectance is very weak; anisotropy is weak without color effects.

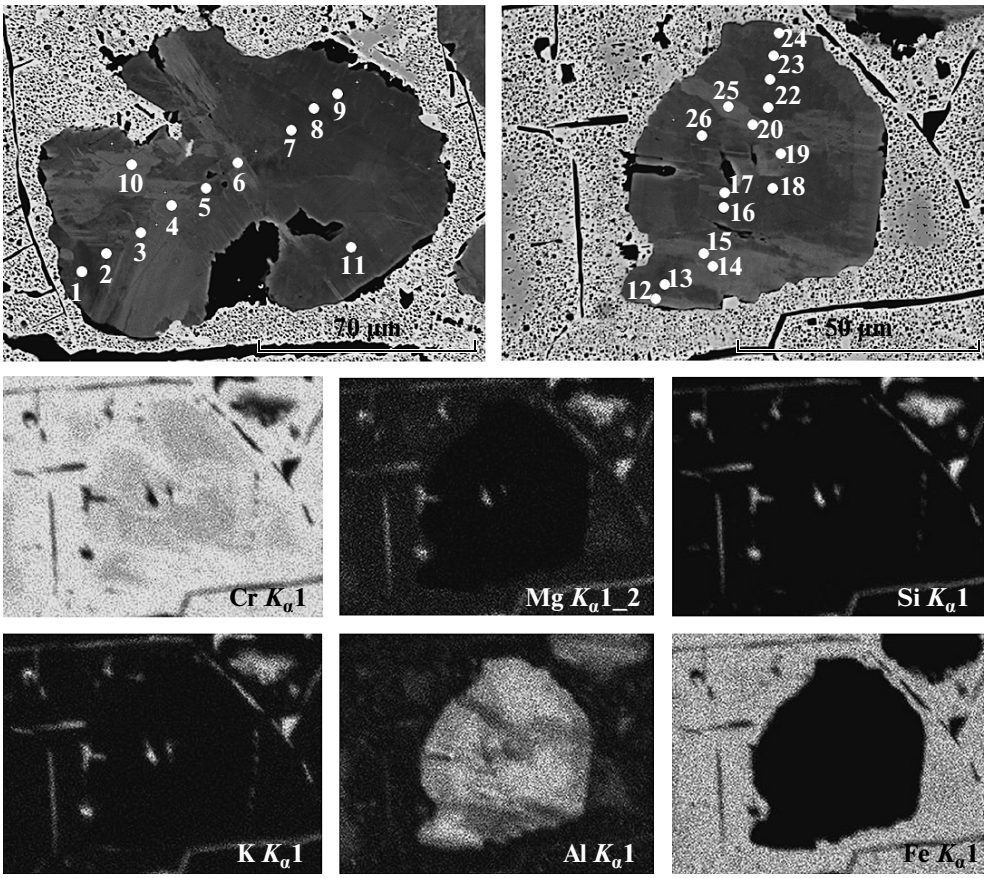

Fig. 8. (a, b) BSE images of mariinskite grains in chromite with lamellar phlogopite and X-ray elemental maps for the grain shown in panel (b); numbers corresponds to Table 3; JCXA-733 JEOL electron microprobe.

The IR spectrum of mariinskite was obtained on a Specord-75 IR spectrometer using micropellets of the mineral placed into a KBr disk; the IR spectrum of chrysoberyl from the Mariinsky deposit was measured under similar conditions (Fig. 7). According to the data of chrysoberyl reported by Plyusnina (1963) and Hofmeister et al. (1987), as well as the data integrated by Povarennykh (1970, 1978) for various minerals, the absorption bands in the IR spectrum of mariinskite within the range 600–1000 cm^{-1} most likely correspond to the stretching vibrations of the BeO_4 tetrahedra and the band in the region of 400–650 cm^{-1} is assigned to the stretching vibrations of $(Cr,Al)O_6$ tetrahedra. The strong band at 1080–1090 cm^{-1} reported in some publications for chrysoberyl corresponds to quartz, which was probably derived from mortar when the mineral was powdered.

CHEMICAL COMPOSITION

The chemical composition of mariinskite was measured with an electron microprobe equipped with EDS and WDS. A total of 92 analyses were performed (Tables 2, 3), among which 20 analyses included a determination of beryllium content with WDS. The measurements were carried out on a Cameca SX 100 electron microprobe equipped with five WD spectrometers at the Institute of Geology and Geochemistry, Ural Branch, Russian Academy of Sciences, Yekaterinburg, analyst – V.V. Khiller. Operating conditions were as follows: an accelerating voltage of 10 kV, a probe current of 100 nA, and beam diameter 2 μm. The following standards were used: Al_2O_3 (Al), TiO_2 (Ti), Cr_2O_3 (Cr), synthetic andradite glass (Fe), and chrysoberyl (Be); all elements were analyzed with analytical line K_α. At the laboratory of the A.E. Fersman Mineralogical Museum, Russian Academy of Sciences, the measurements were performed on a JCXA-733 Superprobe JEOL electron microprobe equipped with five WD spectrometers and an INCA Energy Oxford EDS; analyst – L.A. Pautov. Operating conditions on EDS were as follows: an accelerating voltage of 20 kV, a probe current of 2 nA, and beam diameter 1 μm, and live time 100 s. The following standards were used: Al_2O_3 (Al), $MnTiO_3$ (Ti), Cr_2O_3 (Cr), Fe_2O_3 (Fe), and V_2O_5 (V); all elements were analyzed with analytical line K_α.

We will dwell on the conditions of Be determination in mariinskite on a Cameca SX 100 electron microprobe, because it is not yet a routine procedure.

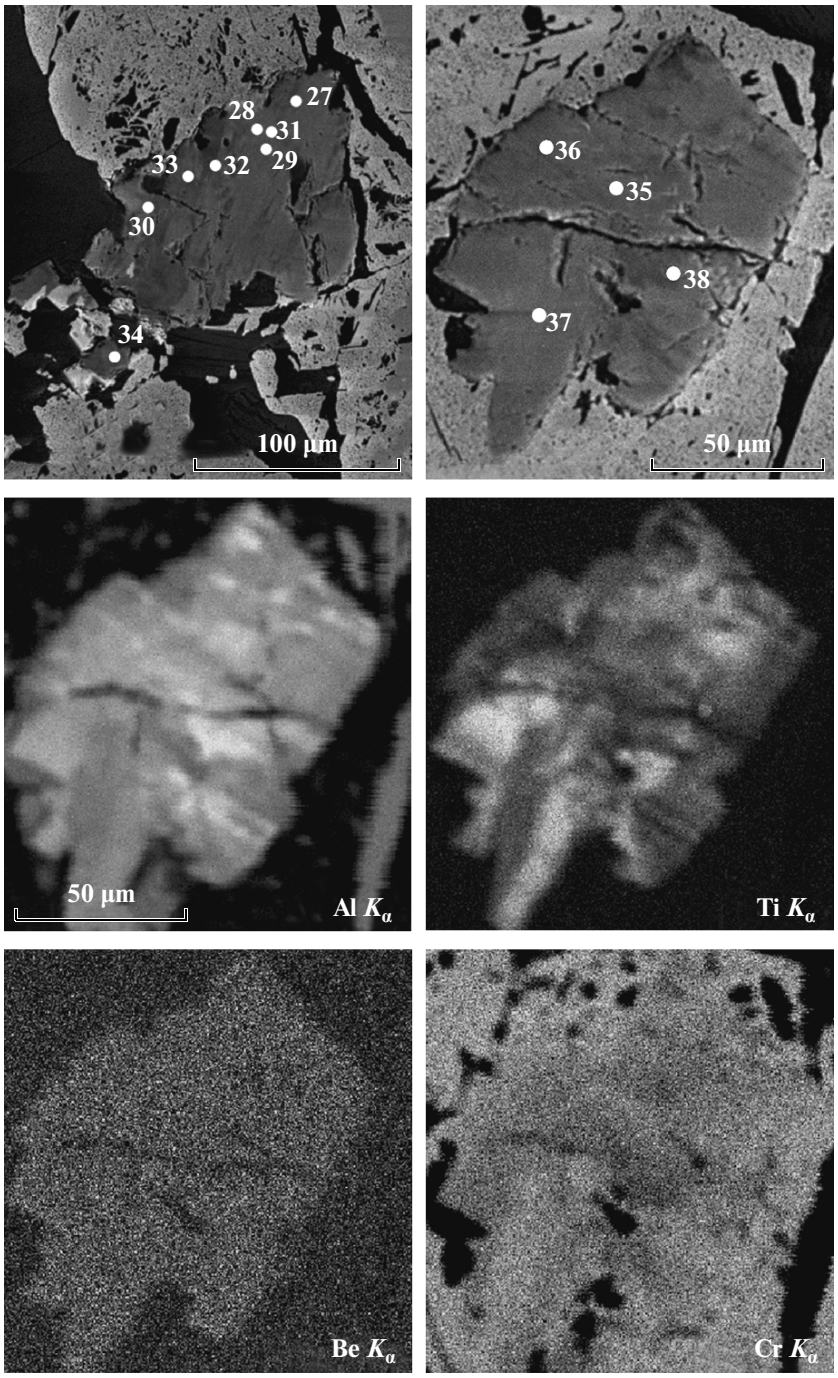

Fig. 9. BSE images and X-ray elemental maps of mariinskite grains, where beryllium was measured on a Cameca SX 100 electron microprobe. Numbers corresponds to that in Table 3.

The studied mineral and standard sample of chrysoberyl were thermally coated by the carbon layer of 250 Å thick. The measurement was carried out at an accelerating voltage 10 kV and a current intensity on the Faraday cylinder 100 nA, using a crystal analyzer PC3 and a gas-flow counter (Ar–CH_4 gas mixture in relationship 9 : 1) with a polypropylene window of 2000 Å; the detector operated in auto differential mode. The position of peak BeK_α(Sin $\Theta \times 10^5$) is 61629; background on the left and right, relative to the peak position, is 8500 and 8620, respectively. Counting time at the peak position and on each side of the peak is 20 and 10 s, respectively. The counting rate at peak BeK_α in the standard sample of chrysoberyl was 31 cps; the counting rate at the background points to the left and to the right of the peak was 19 and 8 cps, respectively. The

Table 2. Chemical composition (wt %) of mariinskite (1–3) and chrysoberyl (4–7)

Component	Mariinskite			Chrysoberyl			
	average	range	$BeCr_2O_4$				$BeAl_2O_4$
	1	2	3	4	5*	6	7
BeO	16.3	15.4–17.2	14.13	18.02	17.50	18.74	19.70
Al_2O_3	23.89	15.24–29.73		78.92	77.07	75.26	80.30
Cr_2O_3	58.67	52.99–65.39	85.87	0.36	0.93	0.30	
Fe_2O_3	0.26	0.11–0.40			3.07	0.31	
FeO	–	–		3.12	–	1.41	
V_2O_3	0.26	0.10–0.39				–	
TiO_2	0.61	0.08–1.80			–	Traces	
SiO_2	–	–		–	–	2.43	
Total	99.98		100.00	100.71	99.14	100.10	100.00

(1) Average of 92 point analyses: 72 analyses were carried out on an EDS (INCA), JEOL JCXA-733 SEM microprobe operated at an accelerating voltage of 20 kv and a probe current of 2 nA, analyst L.A. Pautov; 20 analyses were performed on a WDS Cameca SX 100 microprobe operated at an accelerating voltage of 10 kV and a probe current of 100 nA; analyst V.V. Khiller. The empirical formula calculated on the basis of four O atoms is $Be_{1.03}(Cr_{1.22}Al_{0.74}Ti_{0.01}Fe_{0.01}V_{0.01})_{1.99}O_4$;

(3) theoretical composition; (4–6) Cr-bearing chrysoberyl, the Urals; bulk chemical analyses:

(4) formula $Be_{0.93}(Al_{1.99}Fe_{0.05}Cr_{0.01})_{2.05}O_4$; total includes 0.29 wt % (CuO + PbO), Avdeev (1842);

(5) formula $Be_{0.92}(Al_{1.98}Fe_{0.05}Cr_{0.02}Cu_{0.01})_{2.06}O_4$; total includes 0.57 wt % CuO, Shubin (1843);

(6) 1.51 CaO, 0.04 SnO_2, and 0.10 H_2O^+, Mn and Mg are not detected; the formula was calculated on the basis of four O atoms

(6) formula $(Be_{0.96}Si_{0.05})_{1.01}(Al_{1.90}Ca_{0.03}Fe^{+2}_{0.03}\ Fe^{+2}_{0.01}\ Cr_{0.01})_{1.98}O_4$; total includes 1.51 CaO, 0.04 SnO_2, and 0.10 H_2O^+ wt %; Mn and Mg were not detected; analyst M.E. Kazakova (Vlasov and Kutukova, 1960);

(7) theoretical composition.

*Shubin (1843) gave mass quantities of oxides calculated to the quantity weighed.

Dash means not analyzed.

concentration was calculated with the X-PHI model. Under these operating conditions, the average detection limit of Be was 1.7 wt %.

Despite some chemical variations in various growth zones and sectors of the mineral (Figs. 8, 9; Tables 2, 3), all compositions are satisfactory normalized to formula $Be(Cr,Al,Fe,Ti,V)_2O_4$ and fall into the field of mariinskite (Fig. 2). The empirical formula calculated on the basis of four O atoms for the average composition of the new mineral is $Be_{1.03}(Cr_{1.22}Al_{0.74}Ti_{0.01}Fe_{0.01}V_{0.01})_{1.99}O_4$. The simplified formula of mariinskite is $Be(Cr,Al)_2O_4$. The idealized formula of the end member is $BeCr_2O_4$.

Mariinskite is stable in acids; it is not dissolved either at room temperature or in boiling HCl, HNO_3, or HF. It is dissolved only when heated in a mixture of chloric and phosphoric acids.

X-RAY CRYSTALLOGRAPHY

Unfortunately, the single crystal X-ray diffraction study of the new mineral did not allow us to determine the crystal structure, because no grains of satisfactory quality have been found; all examined grains were irregular intergrowths of twined individuals. E.V. Sokolova determined the orthorhombic unit-cell dimensions from the single crystal X-ray diffraction data: $a = 9.709(2)$, $b = 5.612(1)$, $c = 4.492(1)$ Å, $V = 244.8(2)$ Å^3.

The X-ray powder diffraction data collected using the Debye–Scherrer and Guinier cameras are given in Table 4. Mariinskite is orthorhombic; space group *Pnma* (similarly to synthetic phase $BeCr_2O_4$, JCPDS-ICDD N 11-0613). The unit-cell dimensions calculated by the least squares method from the X-ray powder diffraction data are as follows: $a = 9.727(3)$, $b = 5.619(1)$, $c = 4.499(1)$ Å, $V = 245.9(3)$ Å^3, $Z = 4$. Note that we adhere the chosen setting because of the convenient comparison of the unit-cell dimensions of mariinskite with those of chrysoberyl and synthetic phase $BeCr_2O_4$ in the setting by Weir and Valkenburg (1960) and Cline et al. (1979); though alternative versions of the unit-cell orientation by Dana or Bragg and Brown (1926) are often used in the literature. We explain the observed variations in the unit-cell dimensions of mariinskite (calculated from the single crystal and powder data) by noting the inevitable difference in the composition of the grain studied on the single-crystal diffractometer and of the averaged sample measured using the Debye–Scherrer method, taking

Table 3. Chemical composition of mariinskite (representative local analyses)

Component	1	2	3	4	5	6	7	8	9	10	11	12	13
Wt %													
BeO*	15.97	15.83	15.15	15.08	15.39	15.03	15.89	15.87	15.74	14.79	15.60	15.45	16.15
Al_2O_3	28.39	26.23	18.46	18.77	21.66	17.45	27.96	29.12	27.17	13.65	24.24	18.48	27.08
Cr_2O_3	53.94	56.35	64.23	63.77	60.60	65.06	54.02	52.71	54.24	68.89	57.81	64.47	57.03
Fe_2O_3	0.32	0.22	0.31	0.00	0.12	0.27	0.17	0.00	0.17	0.27	0.21	0.58	0.27
V_2O_3	0.35	0.33	0.28	0.26	0.20	0.23	0.34	0.24	0.19	0.38	0.35	0.20	0.14
TiO_2	0.18	0.26	0.00	0.00	0.00	0.37	0.36	0.40	0.45	0.33	0.00	0.71	0.40
Total	99.15	99.22	98.43	97.88	97.97	98.41	98.73	98.34	97.96	98.31	98.21	99.89	101.07
Formula coefficient calculated on the basis of 4 O atoms													
Be^{+2}*	1.00	1.00	1.00	1.00	1.00	1.00	1.00	1.00	1.00	1.00	1.00	1.00	1.00
$A1^{+3}$	0.87	0.81	0.60	0.61	0.69	0.57	0.86	0.90	0.85	0.45	0.76	0.59	0.82
Cr^{+3}	1.11	1.17	1.39	1.39	1.30	1.42	1.12	1.09	1.14	1.53	1.22	1.38	1.16
Fe^{+3}	0.01	0.00	0.01	0.00	0.00	0.01	0.00	0.00	0.00	0.01	0.00	0.01	0.01
V^{+3}	0.01	0.01	0.01	0.01	0.00	0.01	0.01	0.01	0.00	0.01	0.01	0.00	0.00
Ti^{+4}	0.00	0.01	0.00	0.00	0.00	0.01	0.01	0.01	0.01	0.01	0.00	0.01	0.01
$\Sigma_{cations}$	3.00	3.00	3.01	3.01	2.99	3.02	3.00	3.01	3.00	3.01	2.99	2.99	3.00

Component	14	15	16	17	18	19	20	21	22	23	24	25	26
Wt %													
BeO*	15.28	15.48	15.87	15.58	15.84	15.12	15.00	15.73	16.01	16.08	15.72	14.79	15.96
Al_2O_3	17.04	18.33	23.82	20.00	27.10	18.89	16.46	25.61	26.85	27.17	23.05	13.45	25.66
Cr_2O_3	66.17	65.17	59.83	63.75	55.49	63.22	66.34	57.03	56.47	56.54	60.46	68.92	57.61
Fe_2O_3	0.24	0.21	0.21	0.00	0.00	0.12	0.28	0.00	0.20	0.20	0.36	0.26	0.15
V_2O_3	0.32	0.30	0.31	0.35	0.26	0.30	0.30	0.30	0.30	0.18	0.22	0.28	0.19
TiO_2	0.60	0.73	0.44	0.73	0.37	0.96	1.01	0.37	0.27	0.29	0.11	0.61	0.41
Total	99.65	100.22	100.48	100.41	99.06	98.61	99.39	99.04	100.10	100.46	99.92	98.31	99.98
Formula coefficient calculated on the basis of 4 O atoms													
Be^{+2}*	1.00	1.00	1.00	1.00	1.00	1.00	1.00	1.00	1.00	1.00	1.00	1.00	1.00
$A1^{+3}$	0.55	0.58	0.74	0.63	0.84	0.61	0.53	0.80	0.82	0.83	0.72	0.45	0.79
Cr^{+3}	1.43	1.39	1.24	1.35	1.15	1.36	1.44	1.19	1.16	1.16	1.27	1.53	1.19
Fe^{+3}	0.00	0.00	0.00	0.00	0.00	0.00	0.01	0.00	0.00	0.00	0.01	0.01	0.00
V^{+3}	0.01	0.01	0.01	0.01	0.01	0.01	0.01	0.01	0.01	0.00	0.00	0.01	0.00
Ti^{+4}	0.01	0.01	0.01	0.01	0.01	0.02	0.02	0.01	0.01	0.01	0.00	0.01	0.01
$\Sigma_{cations}$	3.00	2.99	3.00	3.00	3.01	3.00	3.01	3.01	3.00	3.00	3.00	3.01	2.99

Component	27	28	29	30	31	32	33	34	35	36	37	38	39
Wt %													
BeO	15.4	16.2	15.8	17.5	15.1	18.2	16.8	15.6	15.5	16.1	16.9	18.2	17.2
Al_2O_3	16.55	16.13	18.23	22.48	16.25	23.02	28.30	58.06	61.14	62.93	65.58	53.67	62.76
Cr_2O_3	64.72	65.52	60.97	58.93	65.07	57.43	53.67	25.86	20.47	19.11	15.38	26.01	17.06
Fe_2O_3	0.23	0.14	0.10	0.09	0.20	0.17	0.19	0.23	1.49	0.86	1.25	1.19	144
V_2O_3	0.29	0.35	0.40	0.31	0.31	0.25	0.27	0.21	0.17	0.12	0.17	0.16	0.11
TiO_2	1.65	1.24	2.97	0.91	1.85	1.61	0.58	0.26	0.35	0.26	0.33	0.32	0.48
Total	98.87	99.54	98.45	100.25	98.78	100.70	99.76	100.20	99.16	99.39	99.57	99.58	99.01
Formula coefficient calculated on the basis of 4 O atom													
Be^{+2}*	1.01	1.05	1.03	1.10	1.00	1.13	1.04	0.98	1.00	1.04	1.10	1.12	1.11
$A1^{+3}$	0.53	0.52	0.58	0.69	0.53	0.70	0.86	1.20	1.30	1.34	1.40	1.09	1.33
Cr^{+3}	1.40	1.40	1.31	1.21	1.41	1.17	1.09	0.80	0.65	0.61	0.49	0.79	0.54
Fe^{+3}	0.00	0.00	0.00	0.00	0.00	0.00	0.00	0.00	0.03	0.02	0.03	0.02	0.03
V^{+3}	0.01	0.01	0.01	0.01	0.01	0.01	0.01	0.00	0.00	0.00	0.00	0.00	0.00
Ti^{+4}	0.03	0.03	0.06	0.02	0.04	0.03	0.01	0.01	0.01	0.01	0.01	0.01	0.01
$\Sigma_{cations}$	2.99	3.01	2.99	3.03	2.99	3.03	3.01	2.99	2.99	3.01	3.02	3.03	3.03

(1–26) points correspond to numbers in Figs. 8a and 8b; EDS (INCA), JEOL JCXA-733 electron microprobe operated at an acceleration voltage of 20 kv and a probe current of 2 nA; analyst—L.A. Pautov; (27–39) points correspond to numbers in Fig. 9; WDS Cameca SX 100 electron microprobe operated at an acceleration voltage of 10 kV and a probe current of 100 nA, analyst—V.V. Khiller; *BeO is calculated.

Table 4. X-ray powder diffraction data for mariinskite

*I*rel %	d_{obs} Å	d_{calc} Å	*hkl*	*I*rel %	d_{obs} Å	d_{calc} Å	*hkl*
4	4.08	4.083	101	2	1.331	1.328	141
9	3.31	3.303	111, 201	1	1.325	1.323	313
5	2.629	2.630	301	2	1.275	1.276	403
5	2.434	2.433	220	1	1.216	1.216	440, 800
4	2.381	2.382	311	1	1.193	1.192	042
2	2.316	2.315	121	1	1.163	1.162	133, 423, 513
6	2.139	2.140	221	1	1.123	1.125	004
		2.139	401	1	1.120	1.118	342
1	1.999	1.999	411	1	1.098	1.096	114, 204
2	1.701	1.702	131, 421, 511	1	1.084	1.084	151
10	1.651	1.652	222	2	1.071	1.070	442, 802
		1.651	402	1	1.020	1.020	450, 830, 143
1	1.587	1.584	412	1	0.924	0.924	334, 604, 650
2	1.525	1.526	331	1	0.905	0.905	651, 742
		1.525	601	1	0.882	0.882	361
2	1.507	1.507	521	2	0.878	0.878	044, 624
1	1.490	1.484	430	1	0.857	0.857	315
1	1.473	1.472	611	2	0.853	0.854	652, 125
3	1.405	1.405	040			0.851	262, 842
		1.404	620				

The data were collected using the Debye–Scherrer DSK-60A camera (diameter 60 mm), CuK_α radiation, Ni filter. The corrections were calculated from separate patterns with quartz and Si.

the heterogeneous composition of the mariinskite individuals into account (Fig. 8; Table 3).

The Gladstone–Dale compatibility index of properties and composition (calculated from the average composition of minerals and unit-cell dimensions determined from the powder data) is excellent $1 - K_p/K_c = 0.019$. Mariinskite is a chromium analog of chrysoberyl. The properties of the new mineral are compared with that of the synthetic phase $BeCr_2O_4$ and chrysoberyl (Table 5).

ORIGIN CONDITIONS

The origin of the mineralization in the Ural Emerald Mines attracted the attention of researchers for many years and has remained controversial until now. Based on the Ural Emerald Mines, Fersman (1940) elaborated a theory of contaminated pegmatites, in terms of which the emerald-bearing veins are regarded as a product of reaction of pegmatite melt and released fluid with ultramafic host rock. Later, this concept was developed and specified in a number of publications (Vlasov and Kutukova, 1960; Beskin and Marin, 1998). Other authors explain the origin of the emerald-bearing phlogopite schists by greisenization (Ginzburg, 1959; Sherstyuk, 1965; Zhernakov, 1976). Kupriyanova (2004) reviewed in detail the controversial issues concerning genesis of the Emerald Mines. However, all researchers agree that the formation of the emerald-bearing veins is directly related to the adjacent Adui and Malyshevo granitic plutons.

The origin of mariinskite is probably related to the late stage of evolution of these granitic plutons. This mineral occurs as metacrysts and as their intergrowths in chromitite metasomatically replaced with micas. Chromitites, which are found rather frequently in talcites and serpentinized ultramafic rocks in the proximity to the Ural Emerald Mines, were apparently altered (probably repeatedly) by fluids derived from the Adui and Malyshevo plutons. Such a fluid flow is usually formed at the final stage of the evolution of granitic plutons and is accompanied by the formation of pegmatite fields (Fersman, 1940; Vlasov and Kutukova, 1960).

Mariinskite is regarded as a typomorphic mineral of metasomatically altered chromitite because it occurs as abundant inclusions in chromite II and is never found in the primary Al-rich chromite I. This is probably caused by the fact that the earlier, Al-rich chromite I is significantly stabler mineral as opposed to the later developing, Al-poor chromite II (Spiridonov et al., 1997), which underwent leaching (see the abundant cavities in chromite II shown in Fig. 3) and

Table 5. Comparative characterization of mariinskite and cognate phases

Parameter	Mariinskite	Synthetic $BeCr_2O_4$	Chrysoberyl
Formula	$Be(Cr,Al)_2O_4$	$BeCr_2O_4$	$BeAl_2O_4$
Space group	*Pnma*	*Pnma*	*Pnma*
a, Å	9.727(3)	9.792	9.404
b, Å	5.619(1)	5.663	5.476
c, Å	4.499(1)	4.555	4.727
V, Å^3	245.9(3)	252.6	243.4
Z	4	4	4
Color	Dark green	Black (dark green in transmitted light)	Colorless, white (Cr-bearing varieties are light green and green)
D, g/cm^3	4.25(2)	4.42	3.69
Optical sign and axes	Biaxial (+)	Biaxial (–)	Biaxial (+)
α	2.05(1)	2.143	1.746
β	2.09(3)	—	1.748
γ	2.15(1)	2.230	1.756
2*V*, degree	80(10)	45	45
Source	This study	Weir, Valkenburg, 1960	Cline et al., 1979

thus provided enrichment of the fluid in Cr. In addition to the prevalence of Cr over Al, the deficiency of Si in the mineral-forming medium facilitates the formation of mariinskite. The Be and Cr used to form mariinskite were derived from F-rich fluids and host chromitite, respectively.

The specimens with mariinskite are deposited in the Fersman Mineralogical Museum, Russian Academy of Sciences, Moscow (registration no. 4159/1) and Ural Geological Museum (registration no. 51158).

ACKNOWLEDGMENTS

We thank V.M. Vydrin for the samples kindly placed at our disposal; E.V. Sokolova for the single-crystal X-ray diffraction study; I.V. Pekov, A.A. Agakhanov, D.I. Belakovsky, N.N. Eremin, and E.M. Spiridonov for discussion and advice; F.C. Hawthorne for improving the English abstract, and A. Cherevan for assistance in obtaining the IR spectrum of the mineral. This study was supported by the Ministry of Education and Science of the Russian Federation (grant no. 16.518.11.7101).

REFERENCES

Avdeev, I.V., On glucine and its compounds, *Gorny Zh.*, 1842, pt. 3, book 9, pp. 361–391.

Avdonin, V.N. and Polenov, Yu.A., *Ocherki ob ural'skikh mineralakh* (Essays on Ural minerals) Yekaterinburg: UGGGA, 2004.

Basilio, M.S., Pedrosa-Soares, A.C., and Jordt-Evangelista, H., Depositos de alexandrita de Malacacheta, Minas Gerais, *Geonomos*, 2000. vol. 8, no. 1, pp. 47–54.

Beskin, S.M. and Marin, Yu.B., Polygenetic rare-metal mineralization in the granitic ore–magmatic systems, *Zap. Vseross. Mineral. O-va*, 1998, vol. 127, no. 2, pp. 41–54.

Bidny, A.S., Mineralogy, age, and genesis of beryllium occurrences in the Ural emerald belt, *Cand. Sci. (Geol.-Mineral.) Dissertation*, Moscow: Moscow State Univ., 2012.

Bragg, W.L. and Brown, G.B. The crystalline structure of chrysoberyl, *Proc. Roy. Soc. London. A*, 1926. vol. 110, no. 573. pp. 34–63.

Bukin, G.V., Matrosov, V.N., Orechova, V.P., et al., Growth of alexandrite crystals and investigation of their properties, *J. Cryst. Growth.*, 1981, vol. 52, pp. 537–541.

Clark, C.M., Hawthorne, F.C., and Ottolini L., Fluordravite, $NaMg_3Al_6Si_6O_{18}(BO_3)_3(OH)_3F$, a new mineral of the tourmaline group from the Crabtree Emerald Mine, Mitchell County, North Carolina: description and crystal structure, *Can. Mineral.*, 2011, vol. 49, pp. 57–62.

Cline, C. F., Morris, R.C, Dutoit M., and Harget, P.J., Physical properties of $BeAl_2O_4$ single crystals, *J. Mater. Sci.*, 1979, vol. 14, pp. 941–944.

Downes, P.J. and Bevan, W.R. Chrysoberyl, beryl and zincian spinel mineralization in granulite-facies Archaean rocks al Dowerin, Western Australia, *Mineral. Mag.*, 2002. vol. 66. pp. 985–1002.

Dudka, A.P., Sevast'yanov, B.K., and Simonov, V.I., Refinement of the atomic structure of alexandrite, *Krystallografiya*, 1985, vol. 30, pp. 605–609.

Eremin, N.I., Atomistic modeling of the crystal structures of minerals, defects, and solid solutions, *Extended Abstract of Doctoral (Chem.) Dissertation*, Moscow: Moscow State Univ., 2009.

Farrell, E.F., Fang, J.H., and Hewnham, R.E. Refinement of the chrysoberyl structure, *Am. Mineral.*, 1963, vol. 48, pp. 804–810.

Fershtater, G.B., Gerdes, A., and Smirnov, V.N., Age and formation history of the Adui granitic pluton, in *Ezhegodnik-2002* (Yearbook-2002), Yekaterinburg: Inst. Geol. Geochem,, Ural Branch, Russian Acad. Sci., 2003, pp. 146–150.

Fersman, A., Über das färbende Pigment der Smaragde, *Dokl. AN SSSR-A*, 1926, no. 2, pp. 24–25.

Fersman, A.E., *Dragotsennye i tsvetnye kamni Rossii. Monografii KEPS* (Precious and gem stones of Russia. Monographs of KEPS), Petrograd: 4th State Typography, 1920.

Fersman, A.E., *Pegmatity, T. 1: Granitnye pegmatity* (Pegmatites, Vol. 1: Granitic pegmatites), Moscow–Leningrad: Akad. Nauk SSSR, 1940.

Fersman, A.E., Emeralds of the Urals, *Priroda*, 1913, December, pp. 91–93.

Fersman, A.E., Files on Emerald mines, in *Izumrudnye kopi na Urale. Sb. statei i materialov. Materialy KEPS* (Proceeding of KEPS: Emerald mines in the Urals), Petrograd: Rus. Acad. Sci., 1923, issue 46, pp. 5–22.

Franz, G., Gilg, H.A., Grundmann, G., and Morteani, G., Metasomatism at a granitic pegmatite-dunite contact in Galicia: the Franqueira occurrence of chrysoberyl (alexandrite), emerald and phenakite: discussion, *Can. Mineral.*, 1996, vol. 34, pp. 1329–1331.

Geology and mineral resources of the states of India. Part IX – Kerala, Geol. Survey India. Miscellaneous Publication, 2005, no. 30.

Gübelin, E. Alexandrite from Lake Manyara, Tanzania, *Gems Gemol.*, 1976, vol. 15, no 7, pp. 203–209.

Ginzburg, A.I., Pneutomatolitic–hydrothermal beryllium deposits, *Geologiya mestorozhdenii redkikh elementov*, 1959, issue 4, pp. 4–13.

Gromalova, N.A., Solution and melt crystallization and comprehensive study of the composition, crystal morphology and properties of chrysoberyl and alexandrite, *Cand. Sci. (Geol.-Mineral.) Dissertation*, Moscow: Moscow State Univ., 2010.

Gromalova, N.A., Eremin, N.N., and Urusov, V.S., Atomistic modeling of the mixing properties and local structure of $Be(Al,Cr,Fe^{III})_2O_4$ solid solutions, *Glass Phys. Chem.*, 2011, vol. 37, no. 3, pp. 293–306.

Henry, D., Novák, M., Hawthorne F.C., et al., Nomenclature of the tourmaline supergroup minerals, *Am. Mineral.*, 2011, vol. 96, pp. 895–913.

Hofmeister, A.M., Hoering, T. C., Virgo D., Vibrational spectroscopy of beryllium aliminosilicates: heat capacity calculations from band assignments *Phys. Chem. Mineral.*, 1987, vol. 14, pp. 205–224.

Krasnobaev, A.A., Fershtater, G.B., Bea, F., and Montero, P., Polygenetic zircons in the Adui batholith, the Central Urals, *Dokl. Earth Sci.*, 2006, vol. 410, no. 7, pp. 1096–1100.

Kupriyanova, I.I. Points of dispute in genesis of the Malyshevo (Mariinsky) beryllium–emerald deposit, the Central Urals, in *Materialy Ural'skoi letnei mineralogicheskoi shkoly-2003* (Proc. Ural summer mineralogical school-2003), Yekaterinburg, 2003, pp. 37–59.

Mallard, M.Er., Sur quelques substances cristallisées préeparées par Ebelmen, *Bull. Soc. Franc. Minéral.*, 1888, vol. 11, no. 8, pp. 305–311.

Merino, E., Villaseca, C., Pérez-Soba, C., and Orejana, D. First occurrence of gahnite and chrysoberyl in an Iberian Hercynian pluton: the Belvís de Monroy Granite (NE Cáceres, Spain), *Revista Soc. Espán. Mineral.*, 2010. vol. 13, no. 10. pp. 159–160.

Newnham, R., Santoro, R., Pearson, J., and Jansen, C., Ordering of Fe and Cr in chrysoberyl, *Am. Mineral.*, 1964, vol. 49, pp. 427–430.

Plaksenko, A.N., *Tipomorfizm aktsessornykh khromshpinelidov ul'tramafit-mafitovykh magmaticheskikh formatsii* (Typomorphism of accessory Cr-spinels of ultramafic–mafic igneous associations), Voronezh: Voronezh State Univ, 1989.

Plyusnina, I.I., Infrared absorbance spectra of beryllium minerals, *Geokhimiya*, 1963, vol. 1, no. 2, pp. 158–173.

Popov, M.P., Zhernakov, V.I., Zolotukhin, F.F., and Samsonov, A.V., *Ural'skie Izumrudnye kopi. Istoriya izucheniya, geologicheskii ocherk, mineralogicheskii kadastr, bibliografiya*, 2nd Ed. (Ural Emerald Mines. History of study, geological essay, mineralogical cadastre, and bibliography, 2nd Ed., Yekaterinburg: UGGGA, 2008.

Povarennykh, A.S. The use of infrared spectra for the determination of minerals, *Am. Mineral.*, 1978, vol. 63, pp. 956–959.

Povarennykh, A.S., Relationship of IR spectra of minerals to crystal chemical factors, *Mineral. Sb.*, 1970, no. 24, pp. 12–29.

Rabadanov, M.Kh. and Dudka, A.P., On localization of impurity chromium ions in alexandrite, *Crystall. Rep.*, 1998, vol. 43. no. 6, pp. 991–994.

Rager, H., Bakhshand-Khiri, A., and Schmetzer K. Investigation of the intracrystalline Cr^{3+} distribution in natural and synthetic alexandrites, *N. Jb. Miner. Mh.*, 1998, vol. 2, pp. 545–557.

Rose G. IV. Beschreibung einiger neuen Mineralien des Urals. 7) Ueber den Chrysoberyll von Ural, *Ann. Phys. Chem.*, 1839, vol. 48, pp. 570–573.

Sakhnov, A.A., Some typomorphic features of Cr-spinels and chrome ores, *Razvedka Okhrana Nedr*, 2008, no. 8, pp. 21–25.

Santoro, R.P. and Newnham, R.E., Magnetic properties of chromium chrysoberyl, *J. Amer. Ceram. Soc.*, 1964. vol. 47, no. 10. pp. 491–492.

Scalvi, R.M.F., Li, M.S., and Scalvi, L.V.A., Thermal annealing-induced electric dipole relaxation in natural alexandrite, *Phys. Chem. Mineral.*, 2005, vol. 31, pp. 733–737.

Schmetzer K., Bank H., and Gübelin, E., The alexandrite effect in minerals: chrysoberyl, garnet, corundum, fluorite, *N. Jb. Miner. Abh.*, 1980, vol. 138, no 2, pp. 147–164.

Schmetzer, K. *Russian alexandrites*, Stuttgart: Schweizbart, 2010.

Schmetzer, K., Stocklmayer, S., Stocklmayer, V., and Malsy A.-K. Alexandrites from the Novello alexandrite–emerald deposit, Masvingo District, Zimbabwe, *Austral. Gemmol.*, 2011, vol. 24, no 6, pp. 133–147.

Sherstyuk, A.I., Sludite's (phlogopite schists') complexes and their classification, *Zap. VMO*, 1965, vol. 94, no. 1, pp. 62–70.

Shubin, P.I., Report of the Yekaterinburg laboratory for the September third, 1842, *Gorny Zh.*, 1843, book III, pp. 269–296.

Smirnov, V.N., Ivanov, K.S., Krasnobaev, A.A., et al., Results of K–Ar dating of the Adui granitic pluton, eastern slope of the Middle Urals, *Litosfera*, 2006, no. 2, pp. 148–156.

Soman, K. and Nair, N.G.K., Genesis of chrysoberyl in the pegmatites of southern Kerala, India, *Mineral. Mag.*, 1985, vol. 49, pp. 733–738.

Spiridonov, E.M., Barsukova, N.S., Baksheev, I.A., et al., Transformation of primary Cr-spinels of ultramafic rocks of the Bazhenovsky, Karabashsky, Shabrovsky, Saranovsky, and Nuralinsky massifs and small bodies of the Berezovskoye and Gumbeiskoye deposits of the Urals, in *Ural'skaya letnyaya mineralogicheskaya shkola-97* (Ural summer mineralogical school-97) Yekaterinburg, 1997, pp. 23–27.

Trindade, N.M., Scalvi, R.M.F., and Scalvi, L.V.A., Cr^{3+} distribution in Al_1 and Al_2 sites of alexandrite ($BeAl_2O_4$: Cr^{3+}) induced by annealing, investigated by optical spectroscopy, *Energy Power Eng.*, 2010, Febr., pp. 18–24.

Urusov, V.S., Gromalova, N.A., Vyatkin, S. V. et al., Study of structural and valence state of Cr and Fe in chrysoberyl and alexandrite with EPR and Mössbauer spectroscopy, *Moscow Univ. Geol. Bull.*, 2011, vol. 66, no. 2, pp. 102–107.

Vertushkov, G.N., Chromite and fuchsite of the Emerald mines, *Tr. Sverdlovsky Mining Inst.*, 1937, issue 3, pp. 11–13.

Vinnik, D.A., Archugov, S.A., Mikhailov G.G., et al., Kiropoulos process for alexandrite single crystal growth with resistive heating, *Doklady Phys. Chem.*, 2008, vol. 420, part 2, pp. 128–129.

Vlasov, K.A. and Kutukova, E.I., *Izumrudnye kopi* (Emerald mines), Moscow: Akad. Nauk SSSR, 1960.

Von Pott, H.A.G. Geschichte und Wissenchaftliche Beschaftigungen der in St. Petersburg gestifteten Russisch-Kaiserlichen Gesellschaft fur die Gesammte Mineralogie von 1817 bis 1842, in *Schriften der in St.-Petersburg gestifteten Russisch-Kaiserlichen Gesellschaft für die Gessammte Mineralogie*, 1842. Bd 1, Abt. 1, pp. 116–129.

Waldschmidt, W.A. and Gaines, R.V., Occurrence of chrysoberyl near Golden, Colorado, *Am. Mineral.*, 1939, vol. 24, pp. 267–271.

Weir, C.E. and van Valkenburg, A., Studies of beryllium chromite and other beryllium compounds with R_2O_3 oxides, *J. Res. Nat. Bur. Stand.-A. Phys. and Chem.*, 1960, vol. 64A, pp. 103–06.

Zhernakov, V.I., *Izumrudnye kopi. Izumrud. Aleksandrit. Fenakit. Ontogeniya i filogeniya* (Emerald mines. Emerald. Alexandrite, Phenakite. Ontogeny and phylogeny), Yekaterinburg: UGGU, 2011.

Zhernakov, V.I., Typomorphic features of phlogopite from the emerald-bearing parts of ultramafic glimmerite veins, in *Mineralogiya i pertographiya Urala* (Mineralogy and Petrography of the Urals) Sverdlovsk: Sverdlovsk Mining Inst, 1976, issue 3, pp. 83–86.

Zolotukhin, F.F., *Mariinskoe (Malyshevskoe) mestorozhdenie izumruda, Sredny Ural* (Mariinskoye (Malyshevo) emerald deposit, the Central Urals), St. Petersburg: St. Petersburg State Univ., 1996.

Zolotukhin, F.F., The emerald distribution in the Malyshevskoe deposit, Russia, *Geol. Ore Dep.,* 1999, vol. 41, no. 5, pp. 398–408.

Translated by I. Baksheev